

Analysis of the Hatch Tuner by the Waft Site of Matter for Dot-Star Pattern on the Alteration Realization System

¹Jeong-Lae Kim and ²Kyung-Seop Kim

¹Department of Biomedical Engineering, ²Department of Faculty of Liberal Arts, Eulji University, 13135 Seongnam, Korea

Abstract: Waft alteration technology is organized the tuner status for dot-star pattern of the Gleam Realization Rate (GRR) and Differential Realization Rate (DRR) on the waft realization morph. The realization rate condition by the waft realization morph is associated with the suffuse tuner system. As to search a dot-star pattern of the hatch alteration we are organized of the waft value with waft layer dot by the suffuse-upper structure. The concept of realization rate is made sure of the reference of gleam rate and differential rate for alteration signal by the waft tuner morph. Moreover, show up a hatch alteration of the GRR-DRR of the medium in terms of the waft-tuner morph and waft dot tuner that is gained the a Waft value of the Far Alteration of the Wa-RM-FA- β_{MED} with 13.12 ± 2.25 units, that was the a Waft value of the Convenient alteration of the Wa-RM-CO- β_{MED} with 8.10 ± 1.35 units, that was the a Waft value of the Flank alteration of the Wa-RM-FL- β_{MED} with 2.84 ± 0.16 units, that was the a Waft value of the Vicinage alteration of the Wa-RM-VI- β_{MED} with 0.46 ± 0.04 units. The suffuse tuner will be to assess at the ability of the waft-tuner morph for the control degree realization rate on the GRR-DRR that is disclosed the hatch gleam and differential morph by the realization rate system. Suffuse realization system will be possible to modify of a morph by the special signal and to count a waft data of suffuse tuner rate.

Key words: Gleam realization rate, waft realization morph, suffuse realization system, suffuse tuner, differential morph, special signals

INTRODUCTION

The express the shape of substance texture is a combination of various elements which are characterized by their specific shape, size and color such as coke, mineral and mine products. These features have a different affect on the form of the material. Show the other, the computer image processing techniques need to prepare the image to isolate the specific feature which describes the optical texture character from the image enable to perform the complex operations (Piechaczek and Mianowski, 2017; Jeffrey, 1998). Especially, roughness surface can be a limiting factor in the speed of cross-country operations of military vehicles. Typically, this places an upper limit on speed for a given terrain roughness, a strong correlation between surface roughness, measured in Root-Mean-Square elevation variation (RMS) (Murphy and Falih, 1986). In this research, it will be shown that using fractal methods to calculate RMS yields consistent results independently of resolution. The difficulty in demonstrating this fact lies in collecting form RMS values for material data-sets

(Goodin *et al.*, 2017). In this study was the tuner status of the waft realization technology that is organized the hatch alteration of the matter for dot-star pattern with gleam and differential variation by the waft realization morph. This gleam and differential value is expressed the Gleam Rate (GR) and Differential Rate (DR) with the realization function that is disclosed to obtain a basis reference from waft layer is displayed a position of the dot-star pattern, make certain of the waft value with suffuse upper layer on the matter. Also, the waft-wavelength is to make sure of the ability of the alteration function with the hatch degree that is merged the gleam realization rate and differential realization rate by the waft realization morph.

MATERIALS AND METHODS

Sequence control procedure: Waft technology is organized the alteration of the star pattern based on the waft layer system. Waft layer are make sure of propagation from the gleam rate and differential rate on suffuse upper layer structure. The realization rate condition by the waft realization morph is show up with

the suffuse tuner system (Fig. 1). As the concept of alteration rate is made certain the reference for variation of upper position side propagation on the waft vibration morph. The waft layer is gained with the side propagation on star layer and is displayed to disclose a dot-star pattern data of suffuse dot layer structure (Kim and Lee, 2011; Choi and Kim, 2016).

The Waft Realization Morph (Wa-RM) is show up the character of dot-star morph on the matter. Suffuse upper layer position activity is analogized the hatch changes through Gleam Upper Rate (GUR). The results of GUR are impinged to be the limit of Waft Tuner Rate (Wa-TR). The Waft Tuner Morph (Wa-TM) is organized of with matter of the waft tuner change in the gleam activity and differential activity. The Wa-RM system is using the serious formation by the Waft Realization Morph System (Wa-RMS). Serious of Wa-RM is using the hatch suffuse rate that is similar to a control waft-tuner by Suffuse Upper Layer Position Technology (SULPT). Hatch waft tuner is organized in the suffuse dot morph that is induced by the Waft Layer (Wa-L) tool. The arithmetic

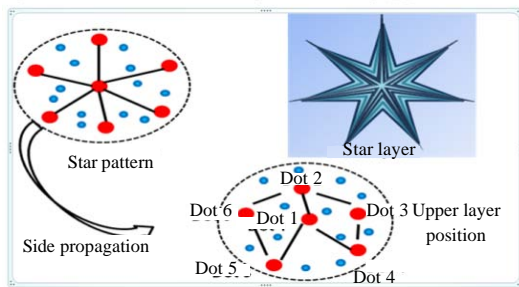


Fig. 1: Waft layer display with the variation of side propagation on the suffuse dot layer structure

character by Wa-RM is induced to the dot of output-limits by the Waft Structure (Wa-S) in the suffuse dot morph. The Waft-Tuner Morph by Wa-RM is using to the dot of output-limits by the Suffuse Realization Rate (SRR) in the Wa-RMS. The Suffuse Dot morph (FODM) was estimated an Upper Tuner Technology (UTT) of side direction from Suffuse Upper Layer (FOUOL) on the SULPT of Wa-RM. The Suffuse Realization Rate Morph (SRRM) is gained suffuse signal from suffuse layer structure mechanisms on the SULPT of Wa-RM. The Waft Gleam Differential Rate (WGDR) is gained the suffuse realization and the suffuse morph on SRR. The SRR is expressed to counter on the hatch suffuse signal by the Suffuse Realization Morph (SRM) (Kim and Kim, 2017a-c) (Fig. 2).

Multiple alignments of Wa-RM upper layer and its evaluation:

Show up the upper layer position score on the Wa-RM is organized with the Overall Vibration Rate (OVR), Far-Convenient Vibration Rate (FCVR) and Flank-Vicinage Vibration Rate (FVVR). These rates are standard deviations that assess the path of point around the side layer from the upper layer of the position and are measured in degrees. The Wa-RM vibration rate scores are gained the displacement for hatch signal in Far-Convenient (FC) and Flank-Vicinage (FV) that display the Wa-FC and Wa-FV. The displacements at upper of layer from FC-axes of horizontal along Wa-FC as x-direction and from FV-axes of vertical Wa-FV along FV-axes as y-direction are evaluated as Wa-RM-FC and Wa-RM-FV, respectively. FCVR can find that the phase of the main layer signal depends both on the propagation channel and the modulating properties of the side layer, which can be both frequency and power-dependent by the Wa-RM-FC. FVVR can measure both amplitude and

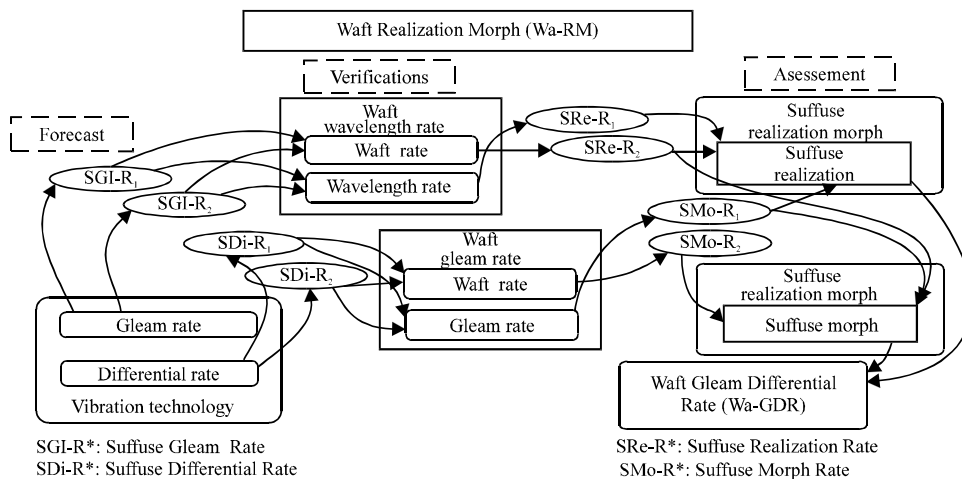


Fig. 2: System block organize waft layer technology by gleam rate and differential rate on suffuse upper layer structure

phase of the disclosed suffuse structure signal as I and Q is the current the far-convenient and flank-vicinage by the Wa-RM-FV. Wa-FC is the modulated carrier of far-convenient on the Wa-RM, Wa-FV is the modulated carrier of flank-vicinage on the Wa-RM, ΔP_{Wa-RM} is amplitude and phase of the received suffuse structure signal of the I_{wa-FC} and Q_{wa-FV} on the Wa-RM (Eq. 1 and 2) (Huiting *et al.*, 2013; Bekkali *et al.*, 2015).

$$\Delta P_{wa-RM} = \frac{I_{wa-FC}^2 + Q_{wa-FV}^2}{Z_0}, \varphi = \arctan \frac{Q_{wa-FV}}{I_{wa-FC}} \quad (1)$$

$$|\Delta \gamma| = \sqrt{I_{wa-FC}^2 + Q_{wa-FV}^2} = \sqrt{\Delta P_{wa-RM} + Z_0} \quad (2)$$

where, Z_0 is the input impedance of the receiver. The indirectly measured upper layer position score data, represented as $\Delta \gamma$ is related to the differential reflection coefficient Wa-RM-FC and Wa-RM-FV can thus be gained as Eq. 3:

$$\angle(\Delta \gamma) = \arctan \frac{Q_{wa-FV}}{I_{wa-FC}} = \varphi \quad (3)$$

Therefore, the test setting that includes the communication range between waft layer pin and their system consist of the properly maintain by the monitoring (Zhang *et al.*, 2017). Suffuse Upper Layer Morph (Su-ULM) is gained a combination scores both Su-ULM-FV and Su-ULM-FC. The Su-ULM-vlaue is calculated from absolute θ -Wa-RM values, so, it is more sensitive to FV-FC and θ -Wa-RM level fluctuations. In general, the θ -Wa-RM-based Su-ULM makes use of the free space propagation model (Eq. 4):

$$\begin{aligned} \theta \text{-Wa-RM}(r)[n.u.] &= \theta_{\text{-Su-ULM-FC}} \gamma / r^{\theta\text{-Su-ULM-FV}} = \\ \theta \text{-Wa-RM}(r)[dB] &= 20 \log_{10} (\theta_{\text{-Su-ULM-FV}}) - \\ \theta_{\text{-Su-ULM-FC}} &20 \log_{10}(r) \end{aligned} \quad (4)$$

Where:

- r = The range or distance
- $\theta_{\text{-Su-ULM-FV}}$ and $\theta_{\text{-Su-ULM-FC}}$ = Coefficients that can be estimated from a non-linear regression that minimizes the Root Mean Square (RMS) by a set of between waft layer

The expression rate of θ -Wa-RM(r) is already linear with respect to $\theta_{\text{-Su-ULM-FV}}$ and $\theta_{\text{-Su-ULM-FC}}$ (Lopez *et al.*, 2017; Chawla *et al.*, 2013).

RESULTS AND DISCUSSION

Properties of the sequence selection: The experiment of Wa-RM-morph is created the Wa-RM- θ_{MAX} , Wa-RM- θ_{MIN}

Table 1: Average of waft structure morphs: the Far GRR-DRR (Wa-RM-FA $\theta_{MAX,AVG}$), Convenient GRR-DRR (Wa-RM-CO $\theta_{MAX,AVG}$), flank GRR-DRR (Wa-RM-FL $\theta_{MAX,AVG}$) and Vicinage GRR-DRR (Wa-RM-VI $\theta_{MAX,AVG}$)

	FA	CO	FL	VI
Average θ	$\theta_{AVG-GRR-DRR}$	$\theta_{AVG-GRR-DRR}$	$\theta_{AVG-GRR-DRR}$	$\theta_{AVG-GRR-DRR}$
Wa-RM- θ_{MED}	13.12±2.25	8.10±1.35	2.84±0.16	0.46±0.04
Wa-RM- $\theta_{MAX,AVG}$	11.45±(-0.46)	3.43±0.19	2.29±0.95	0.29±0.13

and Wa-RM- θ_{AVG} database which are collected from the waft signal tuner morph by the Wa-RM activities (Table 1). Waft signal tuner morph data are used MATLAB 6.1 for the calculations (Kim and Kim, 2017b).

Improvements of multiple sequence selections: Waft Realization Morph (Wa-RM) is made sure of the tuner status for dot-star pattern of the Gleam Rate (GR) and Differential Rate (DR) on the Tuner Technology (WT) condition. WT is to fix the hatch objects of the Waft Gleam Rate (Wa-GR) on the Wa-rm-morph. And WT is to maintain the equivalent things of the Waft Differential Rate (WDR) on the Wa-RM-morph. The results are made sure of the Waft Realization Morph System (Wa-RMS) in accordance with the limit of Gleam Realization Rate (GRR).

Comparison database of GRR-DRR on the Wa-RM- θ_{MAX} , Wa-RM- θ_{MIN} and Wa-rm- θ_{AVG} : Waft Realization Morph (Wa-RM) on the Far (FA- θ) condition is to be show a Gleam Realization Rate-Differential Realization Rate (GRR-DRR) value for the Wa-RM-FA- θ_{MAX} , Wa-RM-FA- θ_{MIN} and Wa-RM-FA- θ_{AVG} (Fig. 3). The large waft of the Wa-RM-FA- θ_{MAX} is to the Flank-Vicinage (FV) direction in the Wa-RMS. Furthermore, Wa-RM activities of far GRR-DRR are the small waft to disparity between the Wa-RM-FA- θ_{MIN} and Wa-RM-FA- θ_{AVG} with the same direction in the Wa-RMS. In the Wa-RM activities of far GRR-DRR is made sure of a very large waft at 26.09±0.77 unit with Wa-RM-FA- θ_{MAX} of the waft structure morph. In the far GRR-DRR of Wa-RM activities is made sure of small waft at 4.70±0.67 unit with Wa-RM-FA- θ_{MIN} in the Wa-RMS. The excellently, this activities of waft structure morph in the far GRR-DRR is to be gained that a waft impinge is happen the FV direction in the Wa-RMS. It is a hatch role in the waft activities of a Wa-RM-Far of far tuner. In the Waft of Wa-RM activities is made sure of a large waft at 14.63±1.23 unit with Wa-RM-FA- θ_{AVG} . Waft Realization Morph (Wa-RM) of Convenient (CO- θ) condition is to be showed up a Gleam Realization Rate-Differential Realization Rate (GRR-DRR) value for the Wa-RM-CO- θ_{MAX} , Wa-RM-CO- θ_{MIN} and Wa-RM-CO- θ_{AVG} (Fig. 3). Wa-RM activities of convenient GRR-DRR are the some waft to disparity between Wa-RM-CO- θ_{MAX} and Wa-RM-CO- θ_{MIN} with the same

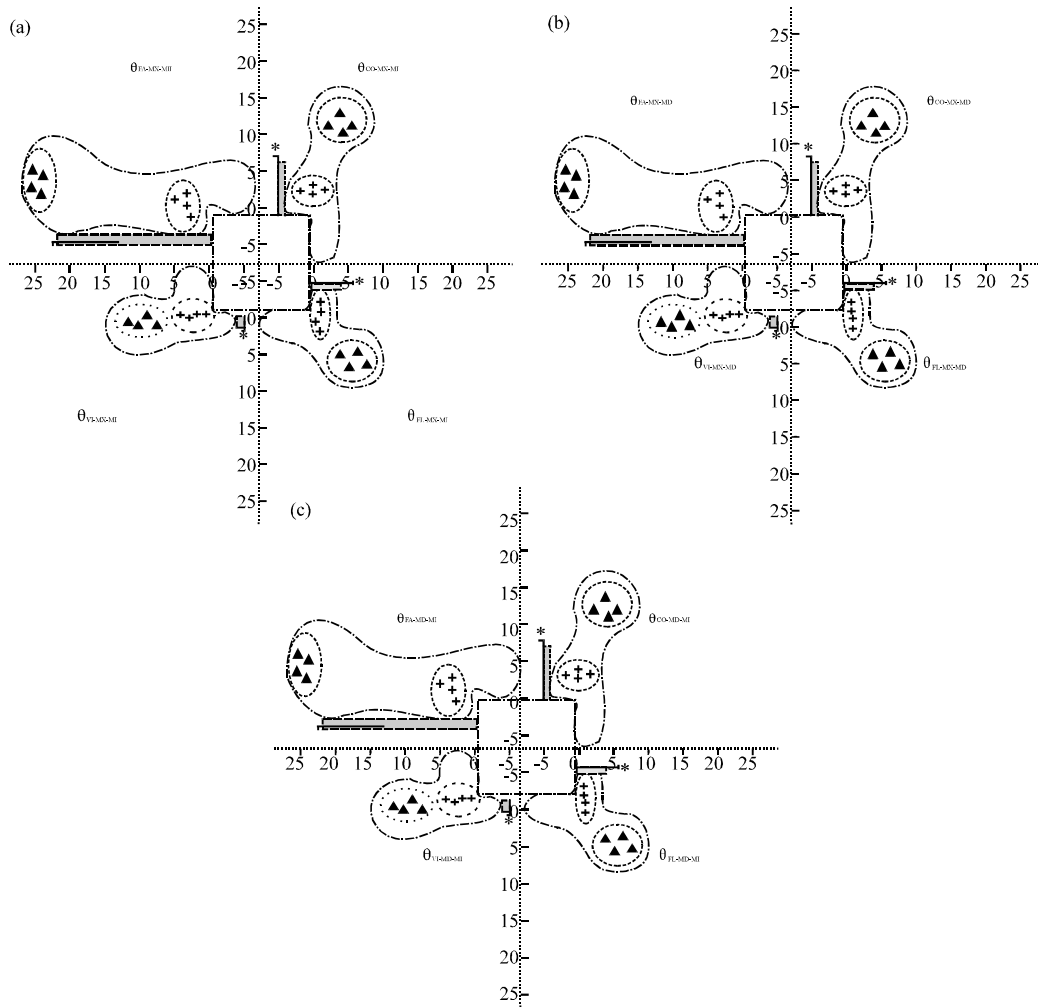


Fig. 3: Wa-RM-morph of the data on the waft condition for activities: a) Limit of the Wa-RM- θ_{MAX} ; b) Wa-RM- θ_{MIN} and c) Wa-RM- θ_{AVG}

direction in the Wa-RMS. Whereas, the Wa-RM activities of convenient GRR-DRR is made sure of small Waft the Wa-RM-CO- θ_{AVG} by the waft structure morph on the FV direction in the Wa-RMS. Wa-RM activities of convenient GRR-DRR is made sure of large waft at 11.71 ± 1.16 unit with Wa-RM-CO- θ_{MAX} of the waft structure morph. In the convenient GRR-DRR of Wa-RM activities is made sure of small at 5.03 ± 0.39 unit with Wa-RM-CO- θ_{MIN} on the FC direction in the Wa-RMS. The excellently, this activities of waft structure morph in the convenient GRR-DRR is to be gained that a waft is happen the same direction in the Wa-RMS. But, it is a hatch role in the waft activities of a convenient tuner. In the waft of Wa-RM activities is made sure of small waft at 8.28 ± 0.97 unit with Wa-RM-CO- θ_{AVG} on the FC direction. The suffice phenomenon of the convenient GRR-DRR is induced serious to vary the Wa-RMS by the suffice structure in

the same direction. Waft Realization Morph (Wa-RM) of Flank (FL- θ) condition is to be showed up a Gleam Realization Rate-Differential Realization Rate (GRR-DRR) value for the Wa-RM-FL- θ_{MAX} , Wa-RM-FL- θ_{MIN} and Wa-RM-FL- θ_{AVG} (Fig. 3). Wa-RM activities of flank GRR-DRR is made sure of small Waft at Wa-RM-FL- θ_{MAX} and Wa-RM-FL- θ_{MIN} of the waft structure morph on the FV direction in the Wa-RMS. Whereas, differently the very small Waft value of Wa-RM-FL- θ_{AVG} is to the FV direction in the Wa-RMS. Wa-RM activities of flank GRR-DRR is made sure of small Waft at 5.58 ± 1.53 unit with Wa-RM-FL- θ_{MAX} of the waft structure morph. In the flank GRR-DRR of Wa-RM activities is made sure of slightly little at 1.43 ± 0.05 unit with Wa-RM-FL- θ_{MIN} on the FC direction in the Wa-RMS. The excellently, this activities of the waft structure morph in the flank GRR-DRR is to be gained that a waft is happen the same

direction in the Wa-RMS. But, it is a hatch role in the waft activities of a flank tuner. In the waft of Wa-RM activities is made sure of small waft at 3.28 ± 0.58 unit with $Wa-RM-FL-\theta_{AVG}$. The suffuse phenomenon of the flank GRR-DRR is induced serious to vary the Wa-RMS by the suffuse structure in the same direction. Waft Realization Morph (Wa-RM) of Vicinage ($VI-\theta$) condition is to be showed up a Gleam Realization Rate-Differential Realization Rate (GRR-DRR) value for the $Wa-RM-VI-\theta_{MAX}$, $Wa-RM-VI-\theta_{MIN}$ and $Wa-RM-VI-\theta_{AVG}$ (Fig. 3). Wa-RM activities of vicinage GRR-DRR is made sure of small Waft at $Wa-RM-VI-\theta_{MAX}$ and $Wa-RM-VI-\theta_{MIN}$ of the waft structure morph on the FC direction in the Wa-RMS. Whereas, differently the small Waft value of $Wa-RM-VI-\theta_{AVG}$ is to the normal direction in the Wa-RMS. Wa-RM activities of vicinage GRR-DRR is made sure of very small waft at 0.80 ± 0.23 unit with $Wa-RM-VI-\theta_{MAX}$ of the waft structure morph. In the vicinage GRR-DRR of Wa-RM activities is made sure of very little at 0.27 ± 0.03 unit with $Wa-RM-VI-\theta_{MIN}$ on the FC direction in the Wa-RMS.

The excellently, this activities of the waft structure morph in the vicinage GRR-DRR is to be gained that a waft is happen the same direction in the Wa-RMS. But it is a hatch role in the waft activities of a vicinage tuner. In the waft of Wa-RM activities is made sure of very small waft at 0.51 ± 0.10 unit with $Wa-RM-VI-\theta_{AVG}$ on the FC direction in the Wa-RMS. The suffuse phenomenon of the vicinage GRR-DRR is induced serious to vary the WA-RMS by the suffuse structure in the normal direction.

CONCLUSION

In this study, hatch variation technology was to organize the vibration realization with the waft realization morph by the waft layer of realization rate. This morph was to be expressed a point of the waft-vibration by the realization rate to gain an alteration data from the basis reference by Gleam Rate (GR) and Differential Rate (DR). As to search a position of the waft layer we are disclosed the waft point with suffuse upper layer on the matter distribution.

Therefore, the waft-vibration was to make sure of the disparity of the alteration morph with the hatch degree that is merged the Gleam Realization Rate and Differential Realization Rate on the GRR-DRR by the waft realization morph system.

ACKNOWLEDGEMENTS

This study is a revised and expanded version of a study entitled "Confirmation of permeate tuner of the

alteration on the matter" presented at Advanced and Applied Convergence Letters with IJCC 2018, Jan. 31-Feb. 7, Hawaii.

REFERENCES

- Bekkali, A., S. Zou, A. Kadri, M. Crisp and R.V. Penty, 2015. Performance analysis of passive UHF RFID systems under cascaded fading channels and interference effects. *IEEE Trans. Wirel. Commun.*, 14: 1421-1433.
- Chawla, K., C. McFarland, G. Robins and C. Shope, 2013. Real-time RFID localization using RSS. *Proceedings of the 2013 International Conference on Localization and GNSS (ICL-GNSS'13)*, June 25-27, 2013, IEEE, Turin, Italy, ISBN: 978-1-4799-0484-6, pp: 1-6.
- Choi, J.S. and J.L. Kim, 2016. A study on institutional types of residents support project for the vitalization of locating locally unwanted land uses in the metropolitan area. *Intl. J. Adv. Smart Convergence*, 5: 47-52.
- Goodin, C., M. Stevens, F.J.V. Rosa, B. McKinley and B. Gates et al., 2017. Calculating fractal parameters from low-resolution terrain profiles. *J. Terramech.*, 72: 21-26.
- Huiting, J., H. Flisijn, A.B. Kokkeler and G.J. Smit, 2013. Exploiting phase measurements of EPC Gen2 RFID tags. *Proceedings of the 2013 IEEE International Conference on RFID-Technologies and Applications (RFID-TA'13)*, September 4-5, 2013, IEEE, Johor Bahru, Malaysia, pp: 1-6.
- Jeffrey, H.J., 1998. Chaos Game Visualization of Sequences. In: *Chaos and Fractals: A Computer Graphical Journey*, Pickover, C.A. (Ed.). Elsevier, Amsterdam, Netherlands, pp: 5-13.
- Kim, J.L. and K.D. Kim, 2017a. Prediction of shiver differentiation by the form alteration on the stable condition. *Intl. J. Internet Broadcasting Commun.*, 9: 8-13.
- Kim, J.L. and K.J. Lee, 2011. A study on the analysis of posture balance based on multi-parameter in time variation. *J. Inst. Internet Broadcast. Commun.*, 11: 151-157.
- Kim, J.L. and K.S. Kim, 2017c. Analysis on the special quantitative variation of dot model by the position transform. *Intl. J. Adv. Culture Technol.*, 5: 67-72.
- Kim, J.R. and H.J. Kim, 2017b. A study of the control structure of the lipid state of stratum on the skin. *J. Convergence Culture Technol.*, 3: 37-42.
- Lopez, Y.A., M.E. Gomez and F.L.H. Andres, 2017. A received signal strength RFID-based indoor location system. *Sens. Actuators A. Phys.*, 255: 118-133.

- Murphy, N.R. Jr. and H.A. Falih, 1986. Comparison of measures of vibration affecting occupants of military vehicles (No. WES/TR/GL-86-18). US Army Corps of Engineers Waterways Experiment Station (WES), USA. <http://www.dtic.mil/docs/citations/ADA178359>.
- Piechaczek, M. and A. Mianowski, 2017. Coke optical texture as the fractal object. *Fuel*, 196: 59-68.
- Zhang, J., G.Y. Tian and A.B. Zhao, 2017. Passive RFID sensor systems for crack detection and characterization. *NDT. E. Intl.*, 86: 89-99.